WATER MOLECULE DYNAMICS IN HYDRATED LYSOZYME

A Deuteron Magnetic Resonance Study

H. PEEMOELLER, F. G. YEOMANS, D. W. KYDON, AND A. R. SHARP
Department of Physics, University of New Brunswick, Fredericton, New Brunswick, Canada E3B 5A3

ABSTRACT Proton nuclear magnetic resonance relaxation investigations of water dynamics in hydrated protein powders have the serious drawback that protein-water intermolecular dipolar interactions make the unambiguous interpretation of the results difficult. To circumvent this difficulty, deuteron spin-lattice and spin-spin relaxation times in lysozyme powder hydrated with deuterium oxide were measured as a function of temperature and at two frequencies. Although the deuteron relaxation results are compatible with a water molecule dynamics model based on either a bimodal distribution of correlation times or anisotropic motion, a comparison of the present results with proton data suggests than an anisotropic motion model is more likely to provide a reasonable description of the water molecule motion. An analysis based on an anisotropic motion model that uses two correlation times to characterize the motion shows that most of the water molecules rotate about their twofold axis of symmetry at a rate that is only ~100 times smaller than the rate of isotropic diffusion in the bulk liquid. The reorientation of the twofold axis of symmetry itself is characterized by a correlation time of $\sim 10^{-7}$ s.

INTRODUCTION

The dynamics of water at the protein-water interface in hydrated protein powders has been widely studied (1–11) using pulsed nuclear magnetic resonance (NMR) relaxation techniques. Such studies commonly use proton resonance, which has a major drawback. The observed proton relaxation rates cannot be used directly to deduce dynamical information about the water because of contributions from the communication or cross-relaxation between protein and water protons. The proton spin-lattice relaxation rates measured ($R_1 = T_1^{-1}$) are a function of the water-protein cross-relaxation rate, as well as the spin-lattice relaxation rates of the water protons (R_{1w}) and the protein protons (R_{1p}). An additional complication is that R_{1w} is itself expected (6) to be a composite of the intrinsic water spin-lattice relaxation rate (R_{1wi}) and an intermolecular spin-lattice relaxation rate contributed by the interface. In addition, the water proton spin-spin relaxation rate R_{2w} can also be influenced by water-protein cross-relaxation effects (4). It is necessary to extract the intrinsic rates R_{1wi} and R_{2wi} from the experimental results in order to obtain information about the water dynamics. These complications often leave the interpretation ambiguous.

An attractive alternative for studying water dynamics is to use deuterated water and observe the deuteron resonance. The deuteron relaxes by means of intramolecular quadrupolar interactions, and the intermolecular effects that complicate the proton experiment are negligible. In this paper, the results of such a deuteron experiment are reported.

It has recently been demonstrated (3, 8, 10) that in wet hen egg white lysozyme (HEWL) samples, the water protons and protein protons are coupled so as to share their coupling to the lattice. For the cross-relaxation mechanism to couple the protein and water protons in this way, the correlation time τ_b characterizing the motion of the water proton-protein proton vector must satisfy $\omega\tau_b \gg 1$ (4), where ω is the resonance frequency used. However, it has also been proposed (7) that near room temperature, the water molecules in hydrated lysozyme move only about two orders of magnitude more slowly than in the bulk liquid at the same temperature. Therefore, the correlation time $\tau_c(w)$ characterizing the motion of the water molecule interproton vector must have magnitude $\tau_c(w) \sim 10^{-10}$ s. For a resonance frequency of 30 MHz, this gives $\omega\tau_c(w) < 1$. This means that whereas the water molecule motion giving rise to R_{1wi} is in the extreme motional narrowing regime, the motion of the intermolecular water proton-protein proton vector giving rise to the coupling across the interface is not.

This all indicates that the description of the water dynamics requires more than one correlation time. The above proposal (7) is of fundamental importance to understanding water dynamics in hydrated proteins. To elu-

D. W. Kydon's permanent address is, Department of Physics, University of Winnipeg, Winnipeg, Manitoba, Canada.

cidate this proposal, we have investigated the temperature dependence of the deuteron T_1 and T_2 in wet HEWL hydrated with D_2O.

EXPERIMENTAL

Grade 1 HEWL and 99.8% D_2O were obtained from Sigma Chemical Co., St. Louis, MO. Paramagnetic impurities were removed from the HEWL as described elsewhere (3, 8).

Deuterated HEWL was prepared by dissolving 0.5 g of the purified HEWL in 10 ml of D_2O. After 8 h, the sample was lyophilized and the powder so obtained was dissolved in 10 ml of fresh D_2O. After a further 8 h, the sample was again lyophilized and the powder was stored in an air-tight container at −5°C. With this procedure, the labile hydrogens removable from HEWL by deuteration are expected to be exchanged. All glassware, including the thin-walled 7.5-mm-o.d. NMR sample tube used for the measurements, was cleaned to remove metal impurities (8).

The wet deuterated HEWL sample was prepared as follows. About 50 mg of the deuterated HEWL powder was placed in a preweighed sample tube. The sample was dried by placing it under vacuum ($\leq 10^{-3}$ Torr) for 12 h. It was then weighed to determine the dry HEWL weight. The vacuum chamber holding the sample was then connected to a second chamber containing D_2O for 20 min before the sample tube was flame-sealed. The sample was found to contain 0.22 g(D_2O)/g(HEWL + D_2O).

Deuteron T_1 and T_2 measurements were performed at 5 MHz and 30.6 MHz using a pulsed NMR spectrometer built in this laboratory. A Nalorac Cryogenics Corp. (Concord, CA) superconducting magnet (30.6 MHz) and a Varian Associates, Inc. (Palo Alto, CA) HA60 magnet (5 MHz) were used. T_1 was measured using the inversion recovery pulse sequence (180°–τ–90°) with typically 20 different values of τ. T_2 was obtained from the shape of the free induction decay (FID). At selected temperatures and at 30.6 MHz, T_2 was also measured with the Carr-Purcell-Meiboom-Gill (CPMG) pulse sequence (12, 13) using a spacing between the 180° pulses of 200 μs. The 90° pulse length was 9.5 μs. Data acquisition, averaging, and analysis were performed with a desk-top computer (9836, Hewlett-Packard Co., Palo Alto, CA) interfaced to a transient waveform recorder (912, Datalab, Mitcham, Surrey, England).

T_1 was measured at 20 different points on the FID using a narrow time window at each point. All recovery curves were found to be exponential and no dependence of T_1 on window position was found. The values of T_1 reported here are averages over all windows. All T_2 decay curves were exponential. Sample temperature was controlled using a standard nitrogen gas flow cryostat and measured by a thermocouple in close proximity to the sample.

RESULTS AND DISCUSSION

The temperature dependence (219–309 K) of water deuteron T_1 and T_2 at 5 MHz and at 30.6 MHz in wet deuterated HEWL is shown in Fig. 1. The deuteron relaxation rates have negligible contributions from intermolecular processes, so that the data (Fig. 1) are taken as the intrinsic deuteron relaxation times, T_{1wi} and T_{2wi}.

Several interesting features in the data (Fig. 1) are noticeable. Consider the T_2 data. Two distinct regions are apparent, with a transition occurring at ~277 K. Each of these regions separately is seen to obey Arrhenius behavior; the correlation time (τ) characterizing the motion is given by:

$$\tau = \tau_0 \exp(E_a/RT), \quad (1)$$

where R is the universal gas constant, E_a is an apparent activation energy, and τ_0 is a pre-exponential factor. With

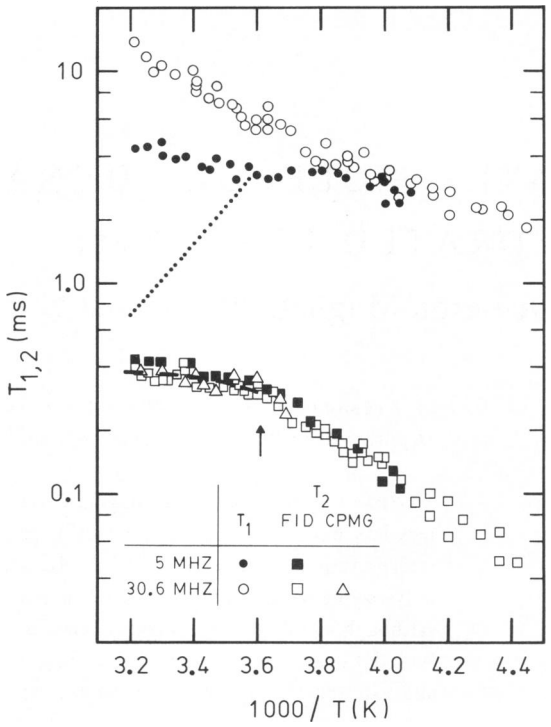

FIGURE 1. Water deuteron T_1 and T_2 in HEWL hydrated with D_2O plotted as a function of $1000/T$. The dashed line was calculated from Eq. 2 (see text for details). The dotted line represents values of C_a^{-1}. The arrow indicates the temperature at which an apparent transition in the T_2 data occurs.

increasing temperature, E_a for the T_2 plot suddenly decreases from ~4.5 kcal/mol for data below 277 K to ~1.0 kcal/mol for data above 277 K (Fig. 1). The most striking feature of the T_2 data is the fact that this transition does not appear to be smooth, but rather is somewhat abrupt and seems to occur at a well-defined temperature.

Although the temperature at which the apparent transition is observed is roughly the same as the melting point of D_2O ice, it does not appear that the transition can be due to the freezing of a free D_2O fraction. At a sufficiently high hydration level, free D_2O would be associated with the HEWL molecule. However, the hydration level of this sample (22%) is well below that required for monolayer coverage (33%), so that there should be no component of free D_2O associated with the lysozyme molecule. The other possibility is that a certain amount of free D_2O not associated with the HEWL in any way was present on the inside walls of the sample tube. This is not reasonable, however, since any such fraction would have T_1 and T_2 such that it would be readily apparent as a separate component in the data. Thus, the change that occurs in the system at ~277 K is not directly associated with the freezing of a free D_2O fraction.

The transverse relaxation times measured using the CPMG sequence (271–309 K) agree with those obtained from the FID (Fig. 1). This agreement shows that effects on the FID caused by macroscopic heterogeneity of the

sample (14) are negligible, and furthermore that the change in E_a of the T_2 data as the temperature is raised above ~277 K is not the result of inhomogeneity in the magnetic field.

The smaller value of E_a of the T_2 plot above 277 K could be the result of the addition of a contribution to R_2 above 277 K from a deuteron fraction that had a relatively short T_2 and that did not contribute to the observed transverse relaxation below 277 K. However, since no shift in T_2 value was observed at 277 K, the process that comes into play above this temperature must have a temperature dependence that is the opposite of that of T_2. We propose that as the temperature is raised above 277 K, an exchange process is suddenly switched on that mixes deuterons between a phase a with T_{2a} observed below 277 K and a phase b in which deuterons have very short T_{2b}, such that they are not observed directly in our experiment.

No shift in T_2 is observed at the transition temperature of 277 K. This implies that immediately above this point, a very slow exchange regime is applicable. In addition, the FID amplitude (corrected for the Boltzman factor) throughout the high-temperature regime was found to be independent of temperature within the limits of experimental uncertainty. These observations suggest that slow exchange between phases a and b occurs over the temperature range 277–307 K. Then the observed transverse relaxation rate for phase a ($1/T'_{2a}$) is approximately given by (15):

$$\frac{1}{T'_{2a}} = \frac{1}{T_{2a}} + C_a, \tag{2}$$

where C_a is the exchange rate for water molecules out of phase a.

Expression 2 was applied to the data (Fig. 1). The dashed line is the calculated T'_{2a} corresponding to the C_a^{-1} values shown in the figure as a dotted line. In this calculation, T_{2a} values were obtained by projecting the T_2 plot below 277 K to higher temperatures. C_a values were found by matching the calculated and observed T'_{2a} at the highest temperature attained in the experiment and assuming that the temperature dependence of C_a is Arrhenius in nature with E_a = 8 kcal/mol (the approximate energy required to break two hydrogen bonds). The calculated line adequately describes the T_2 temperature behavior in this region (Fig. 1).

The deduction that deuterons in phase b have very short T_2 implies that their T_1 is relatively long (see reference 16). Deuterons on a water molecule whose dynamics are in the rigid lattice regime would have such properties. The number of such water molecules hydrated onto a HEWL molecule must be very small compared with the number constituting a monolayer. This is known from the fact that, within experimental error, all deuterons in the sample are being observed. It can now be understood why no effect on the T_1 is caused by the proposed exchange. The exchange times would be short compared with T_1 for most of the data above 277 K, so that the observed relaxation rate R_1 is the sum of the spin-lattice relaxation rates of the a and b phases (R_{1a} and R_{1b}) weighted according to their size fractions. Since both R_{1b} and the size of phase b are much smaller than the corresponding values for phase a, essentially R_{1a} is observed throughout the complete temperature range studied (Fig. 1).

At this time, it is understood neither why the exchange mechanism proposed switches on nor why it does so at approximately the melting point of D_2O ice (~277 K). However, one might speculate that a water-lysozyme cooperative mechanism is involved.

Values of T_{2wi} below ~277 K and the values of T_{1wi} (Fig. 1) appear to be unaffected by the exchange process discussed above. This prompts us to consider these data as constituting the phase a data set. For the following discussion, the relaxation times of this major phase will be referred to simply as T_1 and T_2.

At both frequencies, T_1 decreases with decreasing temperature (Fig. 1). This would suggest that the relaxation is on the high-temperature side of the T_1 minimum and that the correlation time τ characterizing the reorientation of the electric field gradient at the site of the nucleus satisfies $\omega\tau \ll 1$. This condition must be applicable to some of the water molecules, or at least to a component of their dynamics. However, the facts that (a) in this temperature range $T_1 \gg T_2$, (b) T_1 (5 MHz) $\neq$ T_1 (30.6 MHz) at the high-temperature end of the data, and that (c) T_1 (5 MHz) has an E_a different from that of T_1 (30.6 MHz) clearly indicate that the water molecule dynamics are complicated and that water molecule motions with $\omega\tau > 1$ are probably also present in this system. At least qualitatively, a, b, and c could be the result of (i) a distribution of correlation times being required to characterize the water molecule dynamics (17), or (ii) the motion being anisotropic (10, 18). If a distribution of correlation times is applicable, then observations b and c would require that the distribution be bimodal in nature.

For a distribution of τ values, the relaxation rates R_1 and R_2 are given by (17):

$$R_1 = \frac{1}{T_1} = \int_0^\infty P(\tau)\, F_1(\tau) d\tau \tag{3}$$

and

$$R_2 = \frac{1}{T_2} = \int_0^\infty P(\tau)\, F_2(\tau) d\tau, \tag{4}$$

where

$$F_1(\tau) = \frac{3\pi^2}{10}(\mathrm{QCC})^2\left[\frac{\tau}{1+\omega^2\tau^2} + \frac{4\tau}{1+4\omega^2\tau^2}\right]; \tag{5}$$

$$F_2(\tau) = \frac{3\pi^2}{20}(\mathrm{QCC})^2\left(3\tau + \frac{5\tau}{1+\omega^2\tau^2} + \frac{2\tau}{1+4\omega^2\tau^2}\right). \tag{6}$$

$P(\tau)$ is the distribution function and QCC is the deuteron quadrupole coupling constant (QCC = 230 kHz for bulk

water [19]). It is known that QCC for water absorbed onto zeolites is indistinguishable from the bulk water value (20). To calculate R_1 and R_2, this is assumed to be true in wet HEWL as well. In addition, the simplest form of bimodal distribution, one for which the distribution function is the sum of two delta functions, was assumed. Then Eqs. 3 and 4 reduce to:

$$\frac{1}{T_{1,2}} = f_s F_{1,2}(\tau_s^d) + (1 - f_s) F_{1,2}(\tau_f^d), \quad (7)$$

where f_s and $(1 - f_s)$ are the fractional populations of deuterons characterized by the two different correlation times, τ_s^d and τ_f^d, respectively. The correlation times are assumed to vary with temperature according to the Arrhenius activation law (Eq. 1). Preliminary applications of Eq. 7 to the data (Fig. 1) indicated that the rate R_2 is essentially controlled by a small fraction (f_s) of deuterons undergoing much slower reorientations with characteristic time τ_s^d relative to the major fraction $(1 - f_s)$ of deuterons having correlation time τ_f^d. This means that, for practical purposes, R_2 is given by the first term on the right-hand side of Eq. 7. Applying this term to the T_2 data, in conjunction with Eqs. 1 and 6, it was found that $E_{as}^d = (4.5 \pm 0.1)$ kcal/mol and $\tau_{os}^d \simeq (3.9 \times 10^{-12}/f_s)$ s (for $0.001 < f_s < 1$).

With the above information, Eq. 7 was fitted simultaneously to the T_1 and T_2 data [T_1 [30.6 MHz], T_1 [5 MHz], and T_2 [30.6 MHz, 5 MHz for T < 277 K]] using a curve-fitting routine (21) with adjustable parameters f_s, τ_{of}^d, and E_{af}^d. The dashed line in Fig. 2 represents the "best fit" with the fitted parameters given in the figure caption. Although calculated T_1 values show some deviation from the data toward higher temperatures, in general, a reasonable correspondence between calculated relaxation times and experimental data exists (Fig. 2). It is important to note that if either or both peaks of the bimodal distribution were allowed to have a finite width, any discrepancy between calculated and experimental results would increase further. In summary, the application of a bimodal distribution model to the data suggests that, at room temperature (293 K), ~6% of the deuterons in the wet HEWL sample have $\tau_s^d \sim 10^{-7}$ s and 94% have $\tau_f^d \sim 10^{-10}$ s.

To investigate the applicability of an anisotropic motion model to the water dynamics in wet HEWL, the details of the anisotropy involved need to be known. To this end, we adopt the model discussed by Shirley and Bryant (10). Water molecules are bound to the HEWL molecule through hydrogen bonds. Two different positions that a water molecule can assume when forming such hydrogen bonds are as follows: (1) the twofold symmetry axis of the water molecule may be colinear with the hydrogen bond, or (2) one of the two deuteron-oxygen bonds of the water molecule may be colinear with the hydrogen bond. It is assumed that the water molecule undergoes relatively fast rotation (characterized by τ_f^a) about the hydrogen bond axis, which in turn reorients more slowly (characteristic time τ_s^a). Then, letting the fraction of water molecules in position 1 and in position 2 be f_1 and $(1 - f_1)$, respectively, the relaxation rates R_1 and R_2 can be expressed (10, 18) in terms of an anisotropic motion model as follows:

$$\begin{aligned} R_{1,2} &= \frac{1}{T_{1,2}} \\ &= f_1[A_1 F_{1,2}(\tau_s^a) + B_1 F_{1,2}(\tau_1) + C_1 F_{1,2}(\tau_2)] \\ &\quad + \frac{(1 - f_1)}{2}[A_2 F_{1,2}(\tau_s^a) + B_2 F_{1,2}(\tau_1) + C_2 F_{1,2}(\tau_2)] \\ &\quad + \frac{(1 - f_1)}{2}[A_3 F_{1,2}(\tau_s^a) + B_3 F_{1,2}(\tau_1) + C_3 F_{1,2}(\tau_2)], \end{aligned} \quad (8)$$

where, for $i = 1, 2, 3$:

$$A_i = \tfrac{1}{4}(3\cos^2\theta_i - 1)^2;$$

$$B_i = 3\sin^2\theta_i \cos^2\theta_i;$$

$$C_i = \tfrac{3}{4}\sin^4\theta_i.$$

$$\frac{1}{\tau_1} = \frac{1}{\tau_s^a} + \frac{1}{\tau_f^a};$$

$$\frac{1}{\tau_2} = \frac{1}{\tau_s^a} + \frac{4}{\tau_f^a}.$$

For the D_2O molecule, $\theta_1 = 52.5°$, $\theta_2 = 75°$, and $\theta_3 = 0°$.

In the temperature range of interest (see Fig. 2) the rate

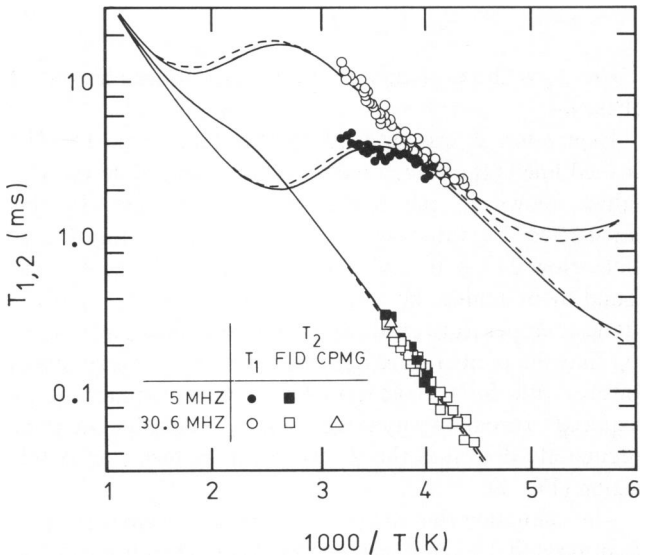

FIGURE 2 Water deuteron T_1 and T_2 as in Fig. 1, except that only the data for the major phase is shown. The dashed line was calculated using the bimodal distribution model (Eq. 7) with fitted parameters $E_{af}^d = (3.2 \pm 0.1)$ kcal/mol, $\tau_{of}^d = (6.9 \pm 0.1) \times 10^{-13}$ s, and $f_s = 0.062 \pm 0.002$. The solid line was calculated using the anisotropic motion model (Eq. 8) with fitted parameters $E_{af}^a = (3.3 \pm 0.1)$ kcal/mol, $\tau_{of}^d = (2.9 \pm 0.1) \times 10^{-13}$ s, and $f_1 = 0.89 \pm 0.01$. A larger range of $1000/T$ values is used here compared with that in Fig. 1 so that the T_1 minimum caused by the slow motion is visible.

$1/T_2$, given by Eq. 8, is essentially controlled by f_1 and $F_2(\tau_s^a)$. Then, in a manner similar to the case of the bimodal distribution model discussed above, we find that $E_{as}^a = (4.5 \pm 0.1)$ kcal/mol and $\tau_{os}^a \simeq 6.4 \times 10^{-12}/(1.005 - f_1)$ s. The relation for τ_{os}^a holds for $0.1 < f_1 < 0.99$. With this information, Eq. 8 was fitted simultaneously to the T_1 and T_2 data (Fig. 2) with adjustable parameters f_1, τ_{of}^a, and E_{af}^a. The resulting fit is shown in Fig. 2 (solid line) with the fitted parameters given in the figure caption. According to this model, all of the water molecules in the sample are hydrogen-bonded to the HEWL molecules; of these water molecules, ~90% are in position 1 and 10% are in position 2. At room temperature, the rotation of the water molecule about a hydrogen bond direction is characterized by $\tau_f^a \sim 10^{-10}$ s. At the same temperature, the reorientation of this "fast rotation axis" proceeds more slowly with a characteristic time $\tau_s^a \sim 10^{-7}$ s.

The quality of the fits of the bimodal distribution model and the anisotropic motion model to the data appear to be similar (Fig. 2). Although the two models have certain features in common (e.g., slow and fast motion mode), they are very different physically. Therefore, it is important to determine which model provides a better description of the water molecule dynamics in wet HEWL.

Confidence that a particular model is applicable would be gained if only that model correctly predicts water proton relaxation rates in an H_2O-HEWL sample. However, it must be kept in mind that such predicted rates are to be compared with the intrinsic water proton rates R_{1wi} and R_{2wi} rather than the observed relaxation rates. In a recent study of cross-relaxation effects in wet HEWL at 40 MHz (22), it was shown that at room temperature the water-HEWL cross-relaxation rate had a value of $\sim 100\ s^{-1}$. This is approximately one-sixth of the observed proton rate R_{2w} but >10 times as large as the observed rate R_{1w} (8). Similar results were found in wet HEWL at 57.5 MHz (10). As a consequence, it is expected that in this system, cross-relaxation effects do not dominate R_{2w} and the observed rate can be taken as an approximate value for R_{2wi}. The proton relaxation rates for the two models discussed above can be calculated using Eqs. 7 and 8, where the factor π^2 $(QCC)^2$ has been replaced with $\gamma^4\hbar^2/r^6$. The quantitites r, $\hbar$, and γ are the water molecule interproton distance, Planck's constant divided by 2π, and the nuclear gyromagnetic ratio (= $2.675 \times 10^4\ G^{-1}\ s^{-1}$ for protons), respectively. Using the parameters given in the legend to Fig. 2, along with r = 1.58 Å, $\theta_1 = 90°$, $\theta_2 = 37.5°$, $\theta_3 = 37.5°$, $\omega/2\pi$ = 40 MHz, and T = 293 K, we find that for the bimodal distribution model $T_1^d(^1H)$ = 120 ms and $T_2^d(^1H)$ = 6 ms. For the anisotropic motion model, we find $T_1^a(^1H)$ = 77 ms and $T_2^a(^1H)$ = 1.5 ms. In an H_2O-HEWL sample having a similar water content as that of the wet HEWL sample used here, the observed T_2 of the water protons at the same temperature and 38 MHz has a value of (1.8 ± 0.1) ms (8). The fact that the observed T_2 is very different from $T_2^d(^1H)$ but nearly the same as $T_2^a(^1H)$ strongly suggests that the anisotropic motion model is applicable here.

Using two-dimensional NMR time evolution correlation spectroscopy, where the magnetization is selectively inverted, it was shown (22) that in the above-mentioned H_2O-HEWL sample at 40 MHz and 293 K, R_{1wi}^{-1} was ~45 ms. Clearly, the correspondence between R_{1wi}^{-1} and $T_1^a(^1H)$ is also better than that between R_{1wi}^{-1} and $T_1^d(^1H)$. This supplies further evidence for the applicability of the anisotropic motion model to the water in wet HEWL.

The above arguments favoring the anisotropic motion model over the isotropic motion model essentially are based on the comparisons of estimated intrinsic water proton relaxation rates for the two dynamical models with such rates estimated in other NMR studies of wet lysozyme. Although the estimates appear to be reasonable, the inherent assumptions do not allow a determination with complete certainty. However, the anisotropic motion model also appears to be reasonable from the following considerations. The hydration level of the sample is below that required for monolayer coverage of the HEWL molecules. Thus, it stands to reason that all of the water molecules of hydration are associated with the HEWL molecules. Such association would be in the form of intermolecular bonds (probably predominantly hydrogen bonds) between a water molecule and a HEWL molecule. It would be expected that a water molecule resides at a hydration site for approximately the lifetime of such a bond. While at such a site, motion about the bond axis will be preferred over the motion of the water molecule axis that is colinear with the bond axis. In essence, this amounts to the water molecule dynamics being anisotropic, which supports the use of an anisotropic motion model.

We believe that the anisotropic motion model is more likely to provide a reasonable description of the water molecule motion. It is of interest to investigate some consequences of this model.

In addition to specifying the details of water molecule dynamics, the anisotropic motion model also provides details about the motion of the water molecules relative to the HEWL molecule. Therefore, it is possible to estimate the magnitude of the water proton–HEWL proton cross-relaxation rate k using this model. In this case, the rate k is given by Eq. 8, where the rates $1/T_{1,2}$ and functions $F_{1,2}(\tau)$ are replaced by k and $F_k(\tau)$, respectively. $F_k(\tau)$ is given by (4):

$$F_k(\tau) = \frac{\gamma^4\hbar^2}{10r^6}\left(\tau - \frac{6\tau}{1 + 4\omega^2\tau^2}\right), \qquad (9)$$

where r is the water proton–HEWL proton distance. Assuming a water molecule–HEWL molecule hydrogen bond length of 2.5 Å (23), it is easily shown that for the water molecule position 1, $\theta_1 = 19.6°$ and r = 2.26 Å. In general, it would be more difficult to assign a value to r for

water molecule position 2. However, it is expected that this distance is considerably larger than 2.26 Å. Since k varies as r^{-6} and only ~10% of the water molecules are in position 2, any contribution to k from these water molecules is assumed to be negligible. Then, using Eq. 8 for k with the parameters found for the anisotropic motion model (legend to Fig. 2) and the above θ_1 and r, we calculate $k = 44\ s^{-1}$ at 40 MHz and 293 K. In a two-dimensional NMR time evolution study of proton magnetization in wet HEWL at the same frequency and temperature, a value for $k = (98 \pm 16)\ s^{-1}$ was deduced (22). Although the two values of k differ by a factor of ~2, the results are nevertheless encouraging. This is because (*a*) the anisotropic motion model probably provides a somewhat oversimplified description of the complex, heterogeneous wet HEWL system and (*b*) any particular water proton may in fact interact, on the average, with more than one HEWL proton (thus the above calculation would yield an under estimated value of k). It should be noted that τ_s^a, which characterizes the motion giving rise to the rate k, is identifiable with the correlation time τ_b discussed earlier.

In summary, it has been shown that deuteron relaxation rates calculated using either a bimodal distribution model or an anisotropic motion model are compatible with the experimental data. However, by taking known proton NMR results into account, it was concluded that the motion of water molecules hydrated onto HEWL is probably anisotropic. According to the anisotropic motion model, ~90% of the water molecules hydrated onto the HEWL have their twofold symmetry axis colinear with the water molecule–HEWL molecule hydrogen bond direction. At room temperature, the rotation of the water molecule about this axis proceeds at a rate that is ~1% that of the rate of rotational diffusion in the bulk liquid and ~1,000 times as large as the rate at which the fast rotation axis reorients.

The value of $E_{as}^a = (4.5 \pm 0.1)$ kcal/mol corresponds to the energy required to break a hydrogen bond. This suggests that the fast rotation axis reorients whenever a water molecule leaves a particular binding site.

More information about the details of molecular interactions and dynamics at the HEWL-water interface should be obtained from a relaxation study of ^{17}O in wet HEWL. This approach is being pursued in our laboratory.

Research funded in part by the Natural Sciences and Engineering Research Council of Canada (NSERC) and by the Research Program Branch of Health and Welfare, Canada.

H. Peemoeller is an NSERC University Research Fellow.

Received for publication 11 December 1984 and in final form 14 June 1985.

REFERENCES

1. Berendsen, H. J. C. 1962. Nuclear magnetic resonance study of collagen hydration. *J. Chem. Phys.* 36:3297–3305.
2. Brey, W. S., Jr., T. E. Evans, and L. H. Hitzrot. 1968. Nuclear magnetic relaxation times of water sorbed by proteins. Lysozyme and serum albumin. *J. Colloid Interface Sci.* 26:306–316.
3. Hilton, B. D., E. Hsi, and R. G. Bryant. 1977. ^1H nuclear magnetic resonance relaxation of water on lysozyme powders. *J. Am. Chem. Soc.* 99:8483–8490.
4. Edzes, H. T., and E. T. Samulski. 1978. The measurement of cross-relaxation effects in the proton NMR spin-lattice relaxation of water in biological systems: hydrated collagen and muscle. *J. Magn. Reson.* 31:207–229.
5. Grigera, J. R., and H. J. C. Berendsen. 1979. The molecular details of collagen hydration. *Biopolymers.* 18:47–57.
6. Fung, B. M., and T. W. McGaughy. 1980. Cross-relaxation in hydrated collagen. *J. Magn. Reson.* 39:413–420.
7. Bryant, R. G., and W. M. Shirley. 1980. Dynamical deductions from nuclear magnetic resonance relaxation measurements at the water-protein interface. *Biophys. J.* 32:3–16.
8. Peemoeller, H., R. K. Shenoy, and M. M. Pintar. 1981. Two-dimensional NMR time evolution correlation spectroscopy in wet lysozyme. *J. Magn. Reson.* 45:193–204.
9. Borah, B., and R. G. Bryant. 1982. Deuterium NMR of water in immobilized protein systems. *Biophys. J.* 38:47–52.
10. Shirley, W. M., and R. G. Bryant. 1982. Proton-nuclear spin relaxation and molecular dynamics in the lysozyme-water system. *J. Am. Chem. Soc.* 104:2910–2018.
11. Winter, F., and R. Kimmich. 1982. NMR field-cycling relaxation spectroscopy of bovine serum albumin, muscle tissue, *Micrococcus luteus* and yeast. *Biochim. Biophys. Acta.* 719:292–298.
12. Carr, H. Y., and E. M. Purcell. 1954. Effects of diffusion on free precession in nuclear magnetic resonance experiments. *Phys. Rev.* 94:630–638.
13. Meiboom, S., and D. Gill. 1958. Modified spin-echo method for measuring nuclear relaxation times. *Rev. Sci. Instrum.* 29:688–691.
14. Funduk, N., D. W. Kydon, L. J. Schreiner, H. Peemoeller, L. Miljković, and M. M. Pintar. 1984. Composition and relaxation of the proton magnetization of human enamel and its contribution to the tooth NMR image. *Magn. Reson. Med.* 1:66–75.
15. Woessner, D. E., and J. R. Zimmerman. 1963. Nuclear transfer and anisotropic motional spin phenomena: relaxation time temperature dependence studies of water absorbed on silica gel. IV. *J. Phys. Chem.* 67:1590–1600.
16. Abragam, A. 1961. The Principles of Nuclear Magnetism. Oxford University Press, Oxford. 264–353.
17. Resing, H. A. 1968. Nuclear magnetic resonance relaxation of molecules adsorbed on surfaces. *Adv. Mol. Relaxation Processes.* 1:109–154.
18. Woessner, D. E. 1962. Nuclear spin relaxation in ellipsoids undergoing rotational brownian motion. *J. Chem. Phys.* 37:647–654.
19. Powles, J. G., and M. Rhodes. 1967. Deuteron spin lattice relaxation in heavy benzene, bromobenzene, water and ammonia. *Proc. Colloq. AMPERE.* 14:757–758.
20. Resing, H. A. 1976. Quadrupole coupling constants in adsorbed water. Effects of chemical exchange. *J. Phys. Chem.* 30:186–193.
21. Bevington, P. R. 1969. Data Reduction and Error Analysis for the Physical Sciences. McGraw-Hill, New York. 204–242.
22. Peemoeller, H., D. W. Kydon, A. R. Sharp, and L. J. Schreiner. 1984. Cross relaxation at the lysozyme-water interface: an NMR line-shape-relaxation correlation study. *Can. J. Phys.* 62:1002–1009.
23. Watenpaugh, K. D., T. N. Margulis, L. C. Sieker, and L. H. Jensen. 1978. Water structure in a protein crystal: rubredoxin at 1.2 Å resolution. *J. Mol. Biol.* 122:175–190.